Copy 581

[redacted]

NASA TM X-567

NASA TM X-567

TECHNICAL MEMORANDUM

X-567

AERODYNAMIC CHARACTERISTICS OF TWO DISK RE-ENTRY CONFIGURATIONS AT A MACH NUMBER OF 2.2

By Frank A. Lazzeroni

Ames Research Center
Moffett Field, Calif.

NATIONAL AERONAUTICS AND SPACE ADMINISTRATION

WASHINGTON May 1961

[redacted]

NATIONAL AERONAUTICS AND SPACE ADMINISTRATION

TECHNICAL MEMORANDUM X-567

AERODYNAMIC CHARACTERISTICS OF TWO DISK RE-ENTRY CONFIGURATIONS AT A MACH NUMBER OF 2.2*

By Frank A. Lazzeroni

SUMMARY

An investigation of the static longitudinal and lateral stability characteristics of models of two possible re-entry vehicles has been made at a Mach number of 2.2. Both models were circular in plan form with elliptic cross sections. One model had a thickness-diameter ratio of 0.325 and a symmetrical section while the other had a thickness-diameter ratio of 0.225, with 2-1/2-percent negative camber.

Both basic shapes were longitudinally unstable about a center of gravity at 40 percent of the diameter from the leading edge. Addition of horizontal-control surfaces, vertical stabilizing surfaces, and a canopy provided static longitudinal and directional stability and positive dihedral effect.

INTRODUCTION

The design of a space vehicle capable of re-entering the earth's atmosphere involves many compromises to cope with the problems of aerodynamic heating, stability and control, vehicle performance, etc., while maintaining adequate usable volume. As a result, both lifting and nonlifting vehicles have been considered and the resulting shapes have been extremely varied (e.g., see refs. 1 through 4). For manned flight, the lifting-type vehicle is especially attractive. One such vehicle receiving consideration is the lenticular shape. This vehicle would enter the atmosphere at a high angle of attack (50° to 90°) to produce high drag and reduce heating; then, as the velocity decreases and the high heating period is passed, the angle of attack would be reduced and the vehicle would enter a gliding phase. It is intended that the vehicle will be landed by more-or-less conventional techniques.

---

*Title, Unclassified

[redacted]

[redacted]

It was recognized that control in low-speed flight could be a problem for the unorthodox disk-shaped vehicle. Accordingly a study was conducted in the Ames 12-Foot Wind Tunnel of this phase of the flight regime of such vehicles (refs. 5 and 6). Out of this study two particular shapes appeared sufficiently promising to warrant some study at supersonic speed and are the subject of the present investigation. These shapes were circular in plan form with elliptic cross sections and incorporated control and stabilizing surfaces at the rear of the vehicle and a canopy. One model had a thickness-to-diameter ratio of 0.325 and a symmetrical section, whereas the other had a thickness-to-diameter ratio of 0.225 and 2-1/2-percent negative camber. Static longitudinal and lateral stability and longitudinal-control characteristics were determined for a Mach number of 2.2 at a Reynolds number of 4×10^6 based on the plan-form diameter. Previous test results for uncambered circular disks have shown stable trim points at high angles of attack at transonic and supersonic speeds (refs. 7 and 8). Lower angles of attack are more appropriate to this speed regime for such vehicles so the present study was confined to angles of attack less than 24°.

NOTATION

The results are presented in standard coefficient form. Lift and drag coefficients are referred to the wind axes; all other aerodynamic coefficients are referred to the body axes. All moments are referred to a point in the longitudinal plane of symmetry on the major axis of the elliptical cross section 0.40 diameter aft of the leading edge. The reference area in each case is the plan-form area of the particular configuration (including the area of the horizontal-control surfaces where appropriate).

C_D drag coefficient, $\frac{\text{drag}}{qS}$

C_L lift coefficient, $\frac{\text{lift}}{qS}$

C_Y side-force coefficient, $\frac{\text{side force}}{qS}$

C_l rolling-moment coefficient, $\frac{\text{rolling moment}}{qSd}$

C_m pitching-moment coefficient, $\frac{\text{pitching moment}}{qSd}$

C_n yawing-moment coefficient, $\frac{\text{yawing moment}}{qSd}$

d diameter

[redacted]

$\frac{L}{D}$ lift-drag ratio

M free-stream Mach number

q free-stream dynamic pressure

R Reynolds number, $\frac{\rho V d}{\mu}$

r radial distance from center of model

S plan-form area of model (including horizontal-control surface area where appropriate)

$\frac{t}{d}$ maximum thickness-to-diameter ratio

V free-stream velocity

y vertical distance from chord plane

α angle of attack, measured with respect to the chord plane

β angle of sideslip

δ horizontal-control surface deflection

ρ free-stream density

μ free-stream viscosity

APPARATUS AND MODELS

The experimental investigation was conducted in the Ames 6- by 6-Foot Supersonic Wind Tunnel which is of the closed-circuit variable-pressure type with a Mach number range from 0.7 to 2.2. Drawings of the models are presented in figure 1, and photographs of the models are shown in figure 2. The basic shapes were circular in plan form with thickness-to-diameter ratios of 0.325 and 0.225 referred to herein as the "thick" model and the "thin" model, respectively. Both models had elliptic profiles; however, the thick model had a symmetrical profile while the thin model had 2-1/2-percent negative camber. The basic shapes were generated by revolving about the minor axis the elliptic sections defined by the coordinates given in table I. The models used in the present investigation were identical to two of those reported in references 5 and 6.

[redacted]

The horizontal-control surfaces were thick flat plates extending radially from the trailing edge of the basic disks as shown in figure 1. Each set of control surfaces consisted of two inboard and two outboard surfaces. The circumferential extent of the outboard surfaces was changed to provide control surfaces of two different sizes (fig. 1(a)). The total area of the horizontal-control surfaces was either 20 or 25 percent of the plan-form area of the basic disks. The hinge lines of the controls were normal to radial lines of the disk at the centers of the respective controls.

The vertical stabilizing surfaces for each model consisted of two constant thickness triangular shapes with rounded leading edges swept back 65°. Each vertical surface was 5-1/2 percent of the plan-form area of the basic disk, giving a total exposed area of 11 percent of the plan-form area. In order to keep the exposed area of the vertical surfaces approximately the same on both models, the exposed span of the vertical surfaces on the thick model was slightly larger (fig. 1).

Details of the model canopies are shown in figure 3. Identical canopies were used for both models. A small fairing was utilized at the rear of the models to accommodate the support sting. An internal six-component strain-gage balance was used to measure the forces and moments on the models.

TEST AND PROCEDURES

Measurements of the static longitudinal and lateral-directional aerodynamic characteristics of the models were made at a Mach number of 2.2 for a Reynolds number of 4 million based on the diameter of the models. The angle-of-attack and angle-of-sideslip ranges were from -6° to $+22^{\circ}$ and the horizontal-control surface deflections were from -10° to $+5^{\circ}$.

Stream Variations

Surveys of the stream characteristics of the wind tunnel have shown that essentially no stream curvature exists in the vicinity of the model and that the axial static-pressure variations are less than 1 percent of the dynamic pressure. Therefore, no corrections for stream curvature or static-pressure variations were made in the present investigation. The data have been corrected to take account of the stream angles in the vertical plane along the tunnel center line measured in these surveys.

[redacted]

[redacted]

Support Interference

Interference from the sting support on the aerodynamic characteristics of the models was considered to consist primarily of a change in the pressure at the base of the model. Accordingly, the static pressures within the balance cavity of the models were measured and the drag data were adjusted to correspond to free-stream static pressure within the cavity and on the base of the annulus of the model fairing around the sting.

Tunnel-Wall Interference

The effectiveness of the perforations in the wind-tunnel test section in preventing choking and in absorbing reflected disturbances at low supersonic speeds has been established experimentally. Unpublished data from the wind-tunnel calibration indicate that reliable data can be obtained throughout the Mach number range of the tunnel if certain restrictions are imposed on the model size and attitude. The configurations used in the present investigation were somewhat larger than are normally tested in this facility; however, shadowgraph observations of the flow around the models substantiated the fact that no choking or reflected disturbances were present for the test conditions reported herein.

RESULTS

The results of the measurements are presented in figures 4 through 8. Figure 4 shows the longitudinal aerodynamic characteristics of the basic disks. The thinner disk had a considerably lower minimum drag, less drag due to lift, and a considerably greater lift-curve slope than the thicker disk. With the center of moments 0.4 diameter aft of the leading edge, the slope of the pitching-moment curve for both models had a positive value at low lift coefficients and decreased to zero at higher lift coefficients.

The aerodynamic characteristics of the complete models with canopy, vertical surfaces, and horizontal-control surfaces having an area of 25 percent of the basic disk area are compared in figure 5. The thinner disk had a considerably lower minimum drag, less drag due to lift, and a greater lift-curve slope. With the moment center 0.4 diameter aft of the leading edge, the pitching-moment curve had a stable slope and the negative camber introduced in the thinner model provided balanced pitching moments at a C_L of 0.1 for a control deflection of 0°. In comparison with the basic disk data of figure 4, the horizontal-control surfaces, vertical surfaces, and canopy provided an increment of dC_m/dC_L of about -0.15.

[redacted]

A comparison of the characteristics of the thinner disk with horizontal-control surfaces of two different sizes is presented in figure 6. The major item of significance is that the aerodynamic center with the larger flaps was about 3 percent of the diameter farther aft than with the smaller flaps.

The aerodynamic characteristics of the thinner model for several deflections of the smaller horizontal-control surfaces are presented in figure 7, and similar data for the thicker model with the larger horizontal-control surfaces are presented in figure 8. The effectiveness of the controls in providing pitching moment at a constant angle of attack was nearly linear for control deflections between $+5^{\circ}$ and -10° and was about the same for both models. The smaller controls on the thin model provided balanced pitching moments to higher lift coefficients for a given control deflection than did the larger flaps on the thick model. This is primarily the result of having camber in the thinner model and also the smaller margin of static stability obtained with the smaller flaps.

The yawing-moment, rolling-moment, and side-force coefficients as a function of angle of sideslip for the various arrangements tested are presented in the (b) parts of figures 5 through 8. As noted in figures 7(b) and 8(b), the vertical surfaces contributed a large degree of directional stability which was not greatly affected by increasing the angle of attack from 0° to 5°. The effective dihedral $-dC_l/d\beta$ was increased by increasing the angle of attack from 0° to 5°. No adverse lateral-directional characteristics were evident.

Ames Research Center
National Aeronautics and Space Administration
Moffett Field, Calif., Apr. 7, 1961

[redacted]

REFERENCES

1. Staff of Langley Flight Research Division (compiled by Donald C. Cheatham): A Concept of a Manned Satellite Reentry Which is Completed With a Glide Landing. NASA TM X-226, 1959.

2. Foster, Gerald V.: Exploratory Investigation at a Mach Number of 2.01 of the Longitudinal Stability and Control Characteristics of a Winged Reentry Configuration. NASA TM X-178, 1959.

3. Eggers, Alfred J., Jr., and Wong, Thomas J.: Re-entry and Recovery of Near-Earth Satellites, With Particular Attention to a Manned Vehicle. NASA MEMO 10-2-58A, 1958.

4. Grant, Frederick C.: Importance of the Variation of Drag With Lift in Minimization of Satellite Entry Acceleration. NASA TN D-120, 1959.

5. Demele, Fred A., and Brownson, Jack J.: Subsonic Longitudinal Aerodynamic Characteristics of Disks With Elliptic Cross Sections and Thickness-Diameter Ratios From 0.225 to 0.425. NASA TN D-788, 1961.

6. Demele, Fred A., and Brownson, Jack J.: Subsonic Aerodynamic Characteristics of Disk Re-entry Configurations With Elliptic Cross Sections and Thickness-Diameter Ratios of 0.225 and 0.325. NASA TM X-566, 1961.

7. Mugler, John P., Jr., and Olstad, Walter B.: Static Longitudinal Aerodynamic Characteristics at Transonic Speeds of a Lenticular-Shaped Reentry Vehicle. NASA TM X-423, 1960.

8. Jackson, Charlie M., Jr., and Harris, Roy V., Jr.: Static Longitudinal Stability and Control Characteristics at a Mach Number of 1.99 of a Lenticular-Shaped Re-entry Vehicle. NASA TN D-514, 1960.

[redacted]

[redacted]

TABLE I.- COORDINATES OF SURFACE OF MODELS
[All dimensions in inches]

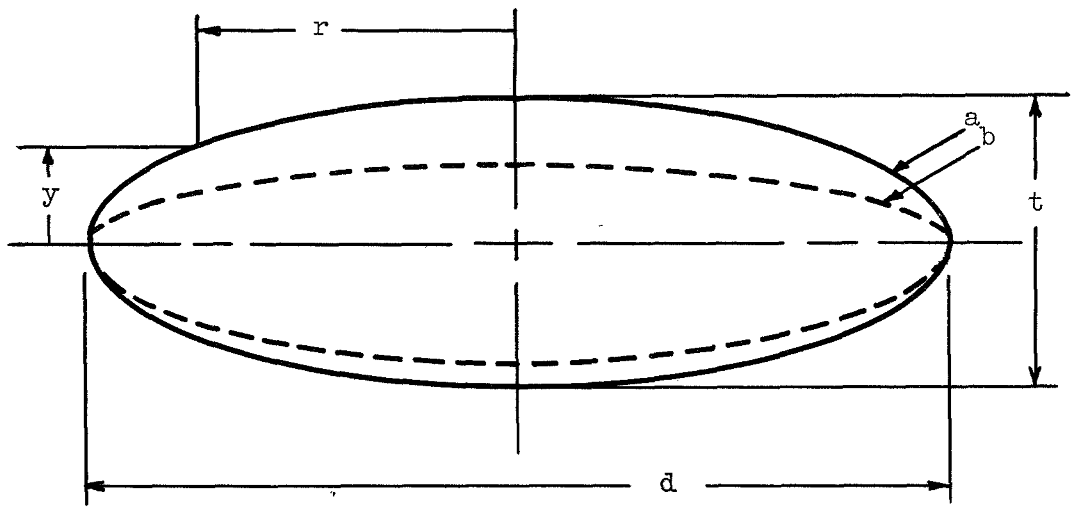

r	t/d = 0.325	t/d = 0.225		r	t/d = 0.325	t/d = 0.225	
	$\pm y_a$	y_b	$-y_b$		$\pm y_a$	y_b	$-y_b$
0	3.90	2.10	3.30	10.00	2.16	1.16	1.82
1.00	3.89	2.09	3.29	10.50	1.89	1.02	1.60
2.00	3.84	2.07	3.25	10.75	1.73	.93	1.47
3.00	3.78	2.03	3.20	11.00	1.56	.84	1.32
4.00	3.68	1.98	3.11	11.25	1.36	.73	1.15
5.00	3.54	1.91	3.00	11.50	1.11	.60	.94
6.00	3.38	1.82	2.86	11.60	1.00	.54	.84
7.00	3.17	1.71	2.68	11.70	.87	.47	.73
7.50	3.04	1.64	2.58	11.80	.71	.38	.60
8.00	2.91	1.56	2.46	11.90	.50	.27	.42
8.50	2.75	1.48	2.33	11.95	.36	.19	.30
9.00	2.58	1.39	2.18	12.00	0	0	0
9.50	2.38	1.28	2.02				

[redacted]

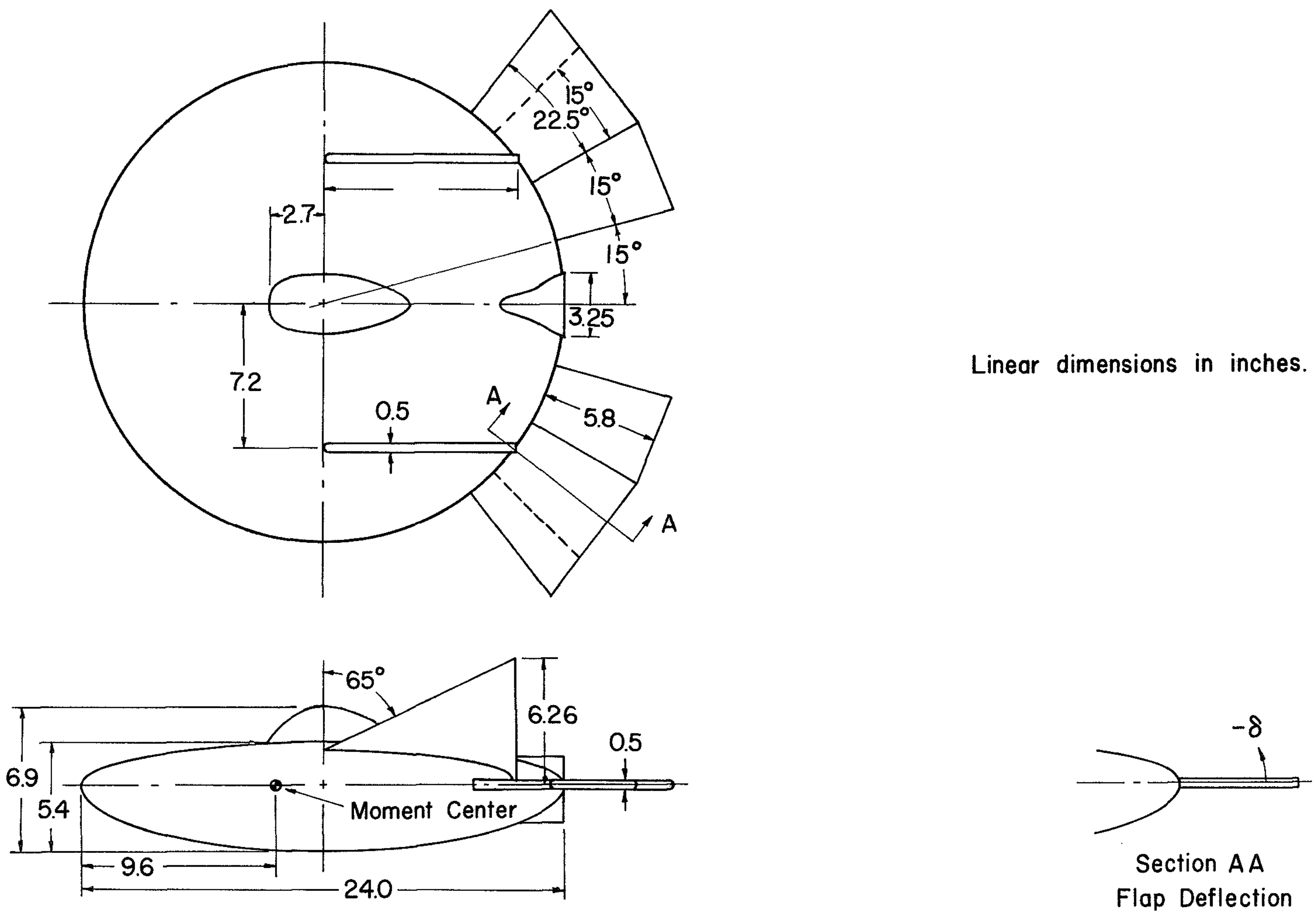

(a) t/d = 0.225

Figure 1.- Dimensional drawings of models.

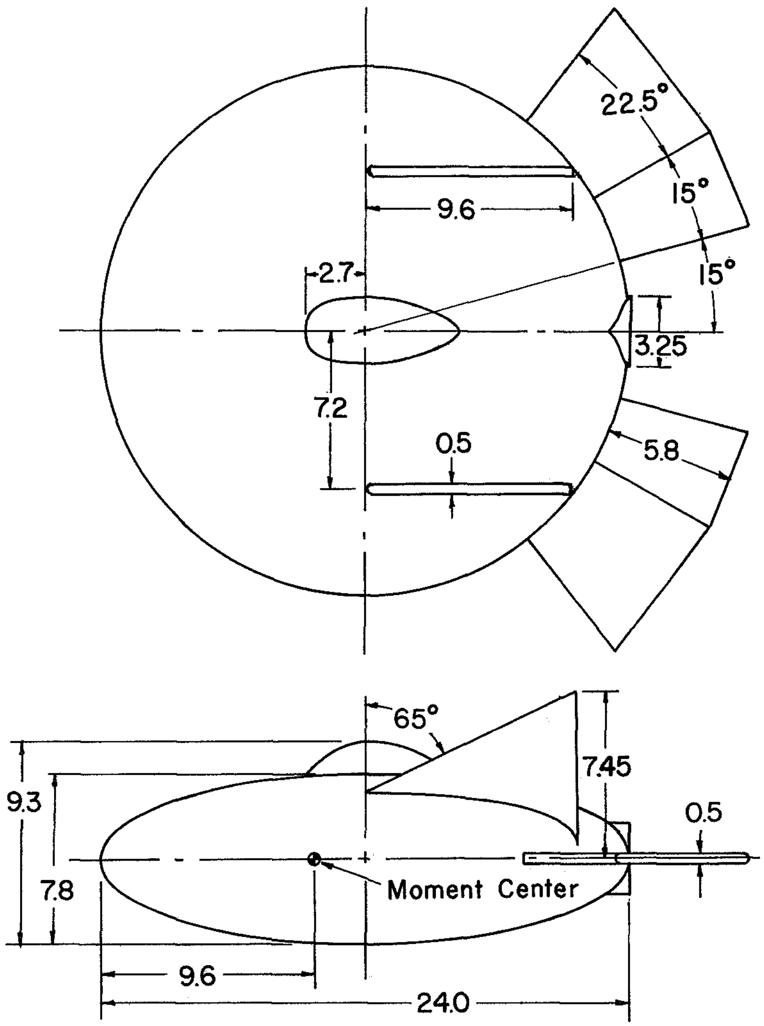

Linear dimensions in inches.

(b) t/d = 0.325

Figure 1.- Concluded.

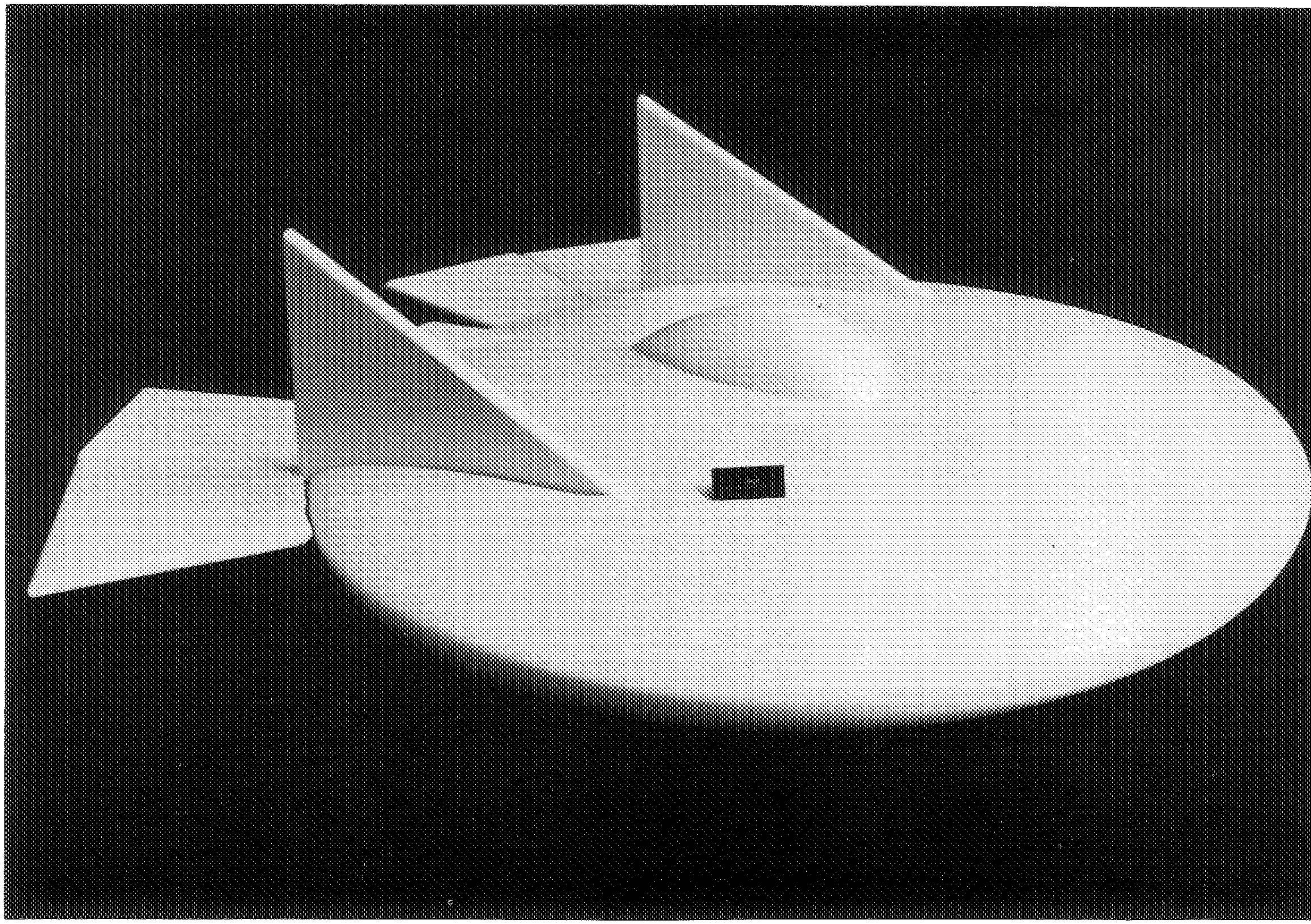

A-27284

(a) t/d = 0.225

Figure 2.- Photographs of models.

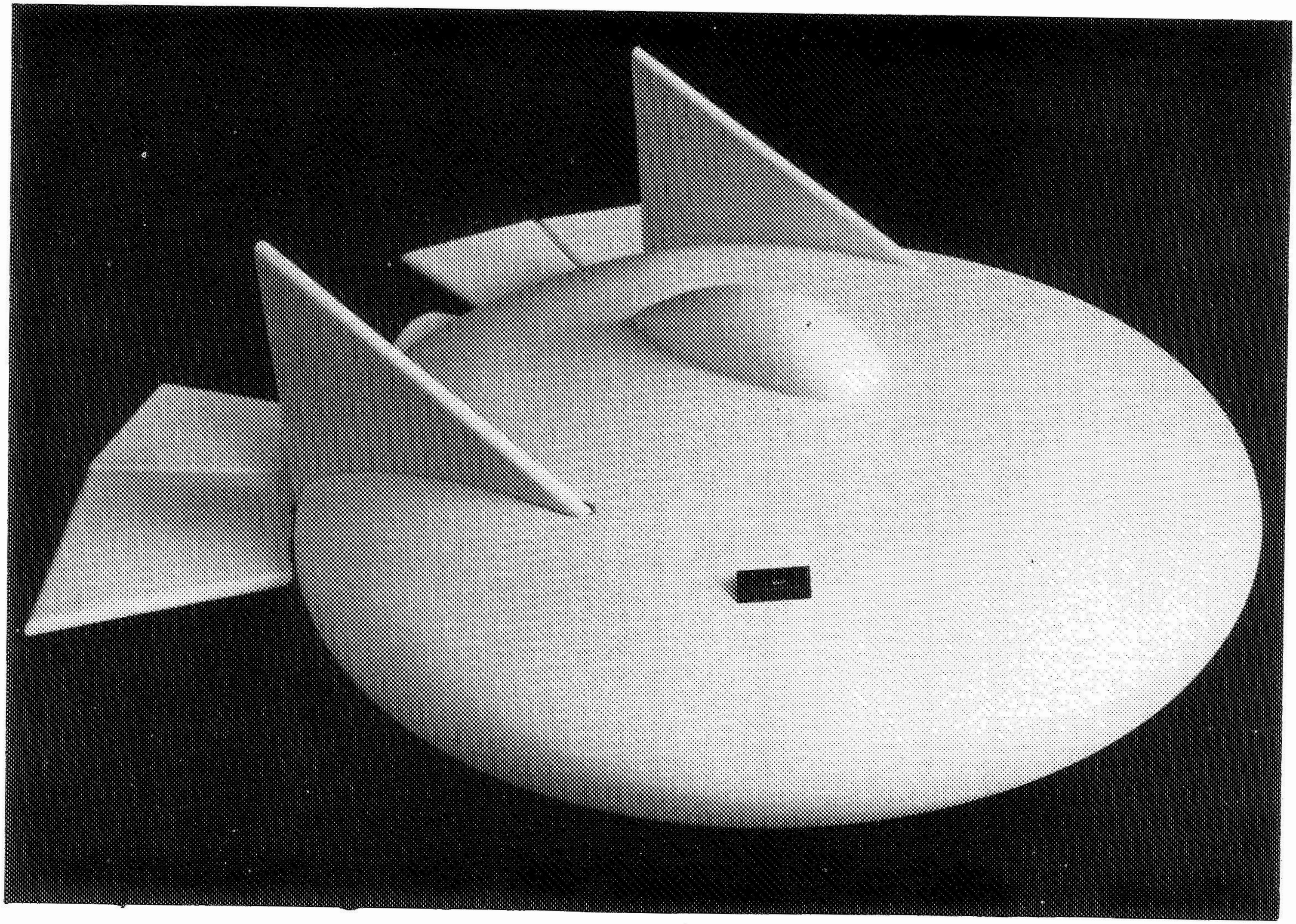

(b) $t/d = 0.325$ A-27282

Figure 2.- Concluded.

[redacted]

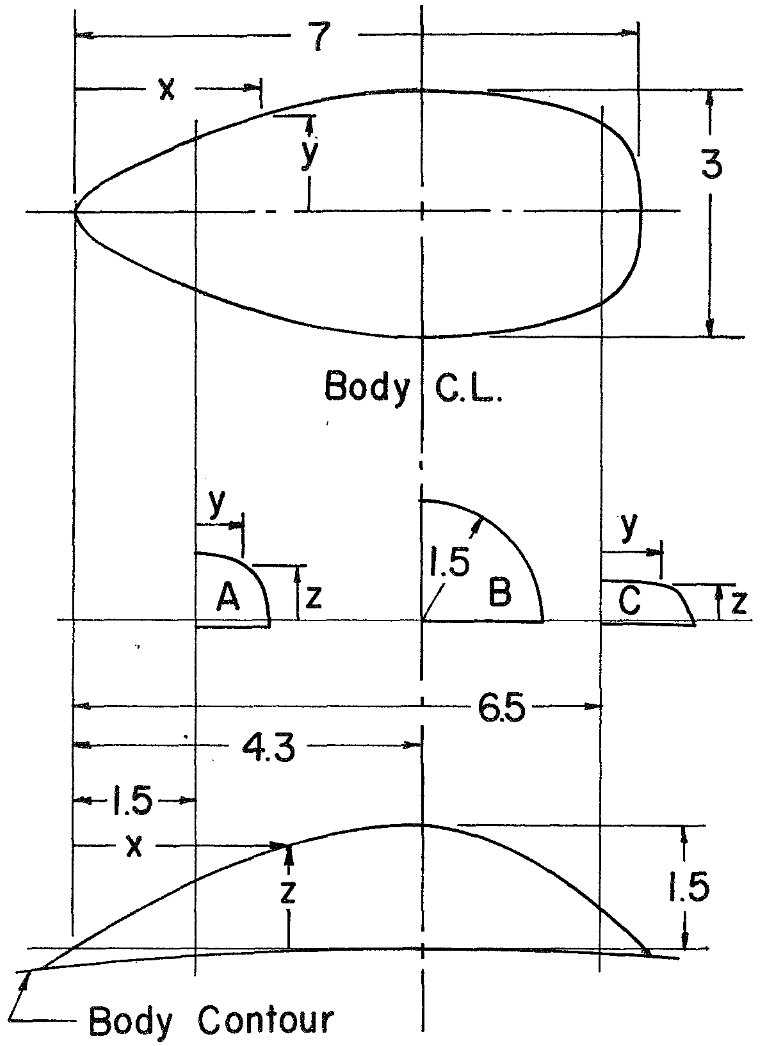

Plan x	Plan y	Profile x	Profile z	Sect. A y	Sect. A z	Sect. C y	Sect. C z
0	0	0	0	0	0.81	0	0.49
0.1	±0.29	1.0	0.58	0.2	.80	0.2	.49
0.5	0.44	2.0	1.04	.3	.79	.4	.48
1.0	0.69	3.0	1.36	.4	.76	.5	.47
2.0	1.09	4.3	1.50	.5	.73	.6	.46
3.0	1.38	5.0	1.36	.6	.68	.7	.44
4.3	1.50	6.0	0.85	.7	.59	.8	.41
5.0	1.47	7.0	0	.8	.47	.9	.36
6.0	1.31			.9	0	1.0	.26
6.5	1.10					1.1	0
6.8	0.82						
7.0	0						

Figure 3.- Canopy details.

[redacted]

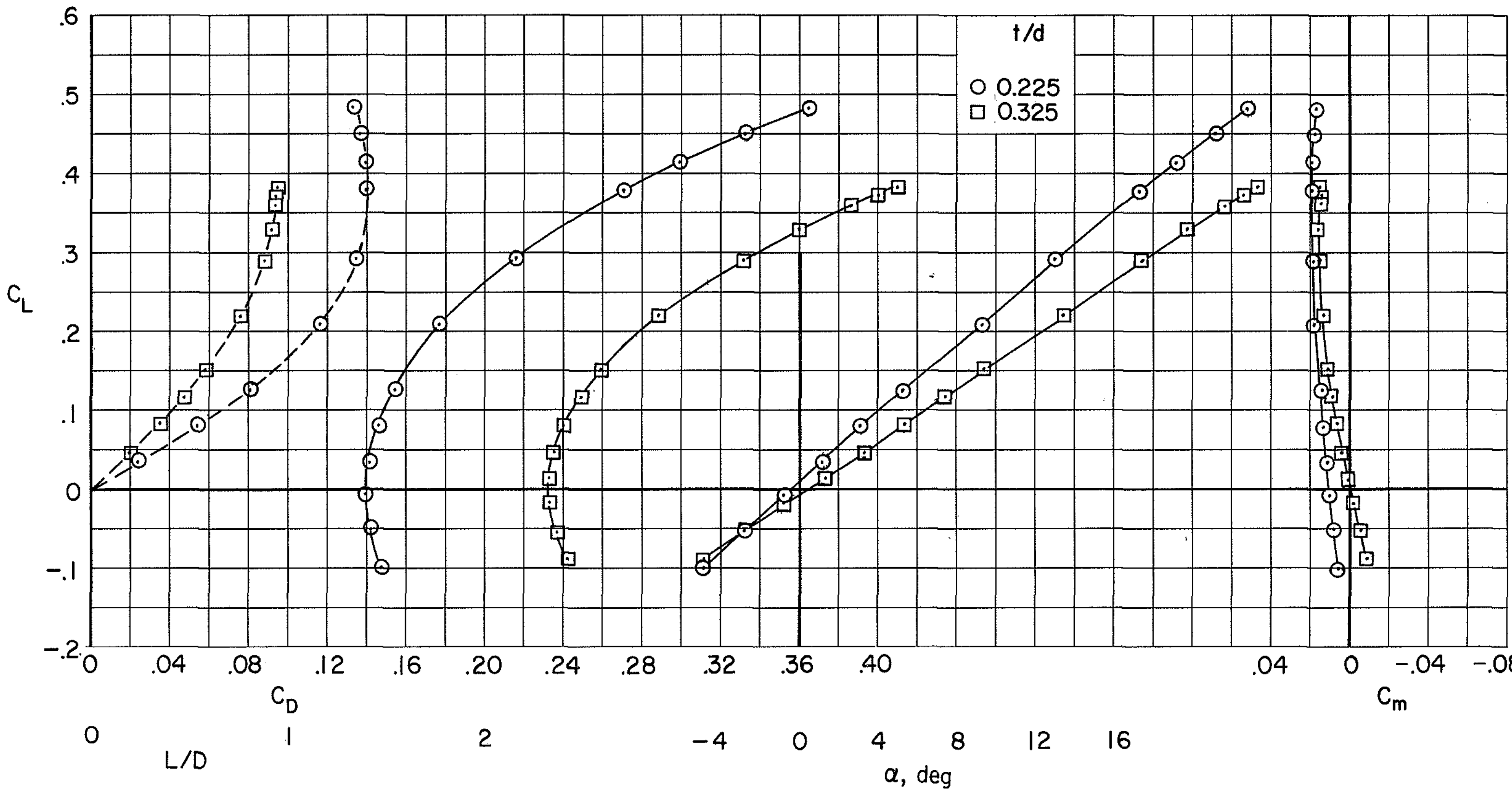

Figure 4.- Static longitudinal aerodynamic characteristics of the basic disks.

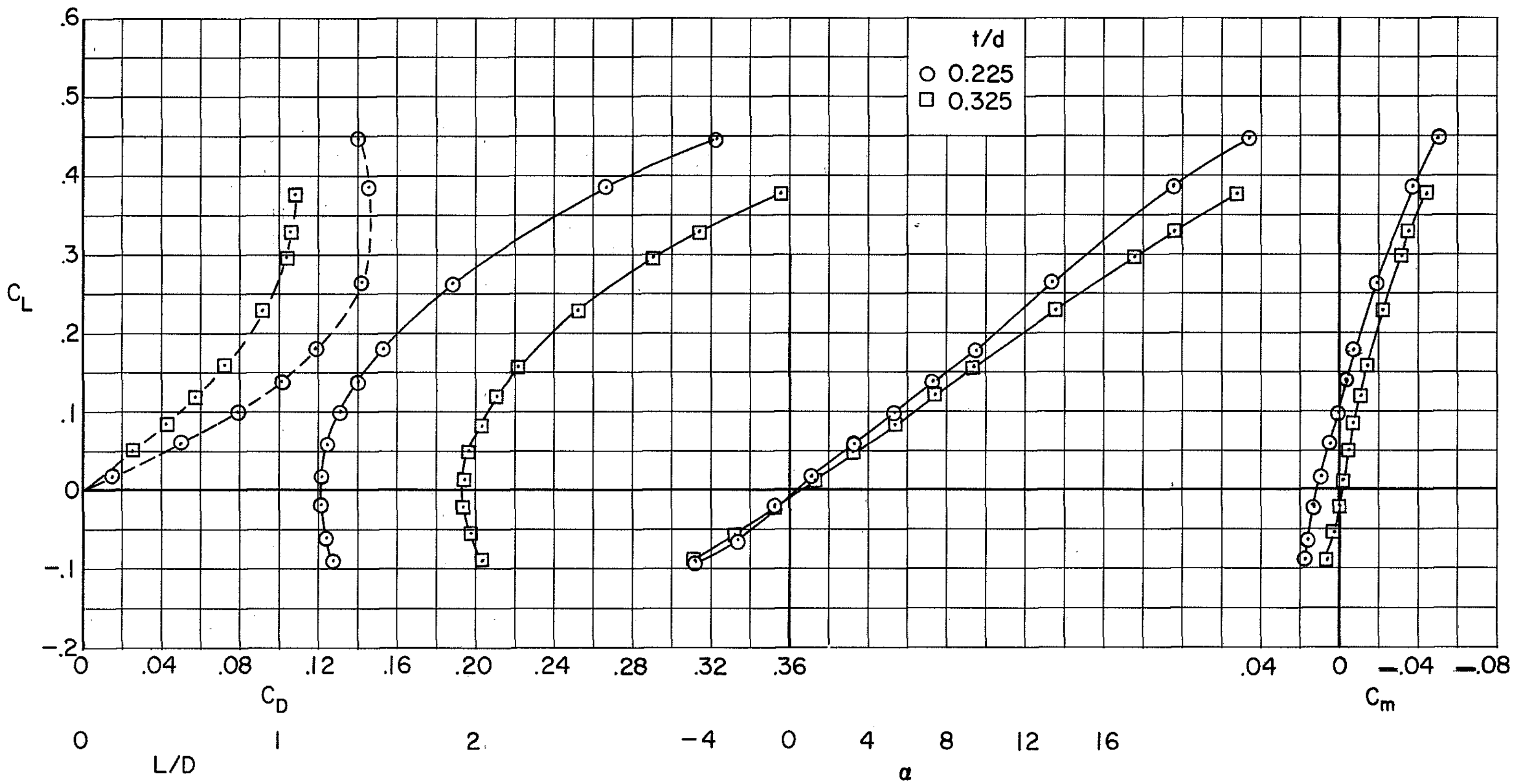

(a) Static longitudinal characteristics.

Figure 5.- Aerodynamic characteristics of the complete models (25-percent-area horizontal-control surfaces undeflected).

[redacted]

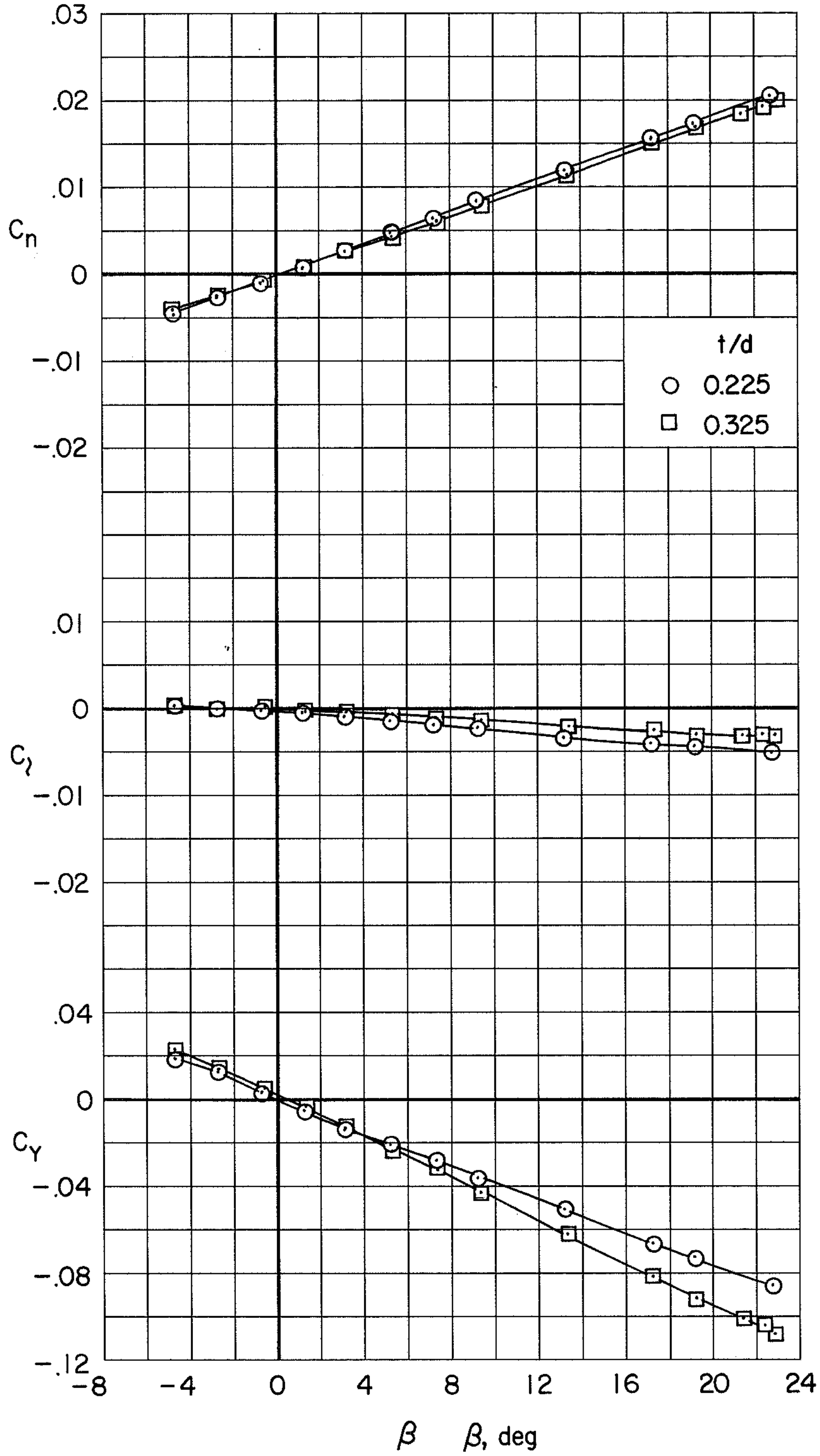

(b) Static lateral-directional characteristics, $\alpha = 0$.

Figure 5.- Concluded.

A
4
8
0

[redacted]

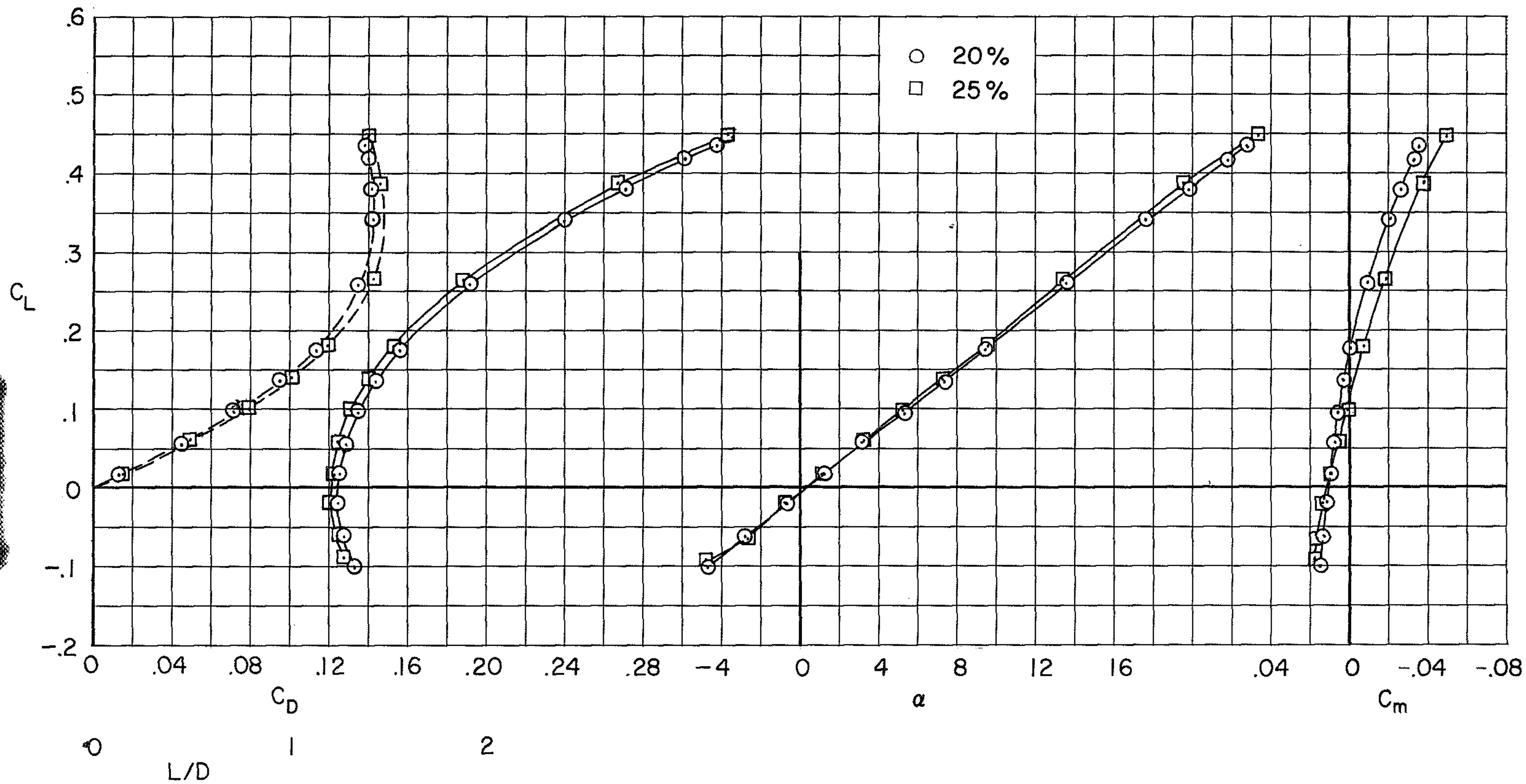

(a) Static longitudinal characteristics.

Figure 6.- Effect of horizontal-control-surface area on the aerodynamic characteristics of the model with thickness-diameter ratio of 0.225.

[redacted]

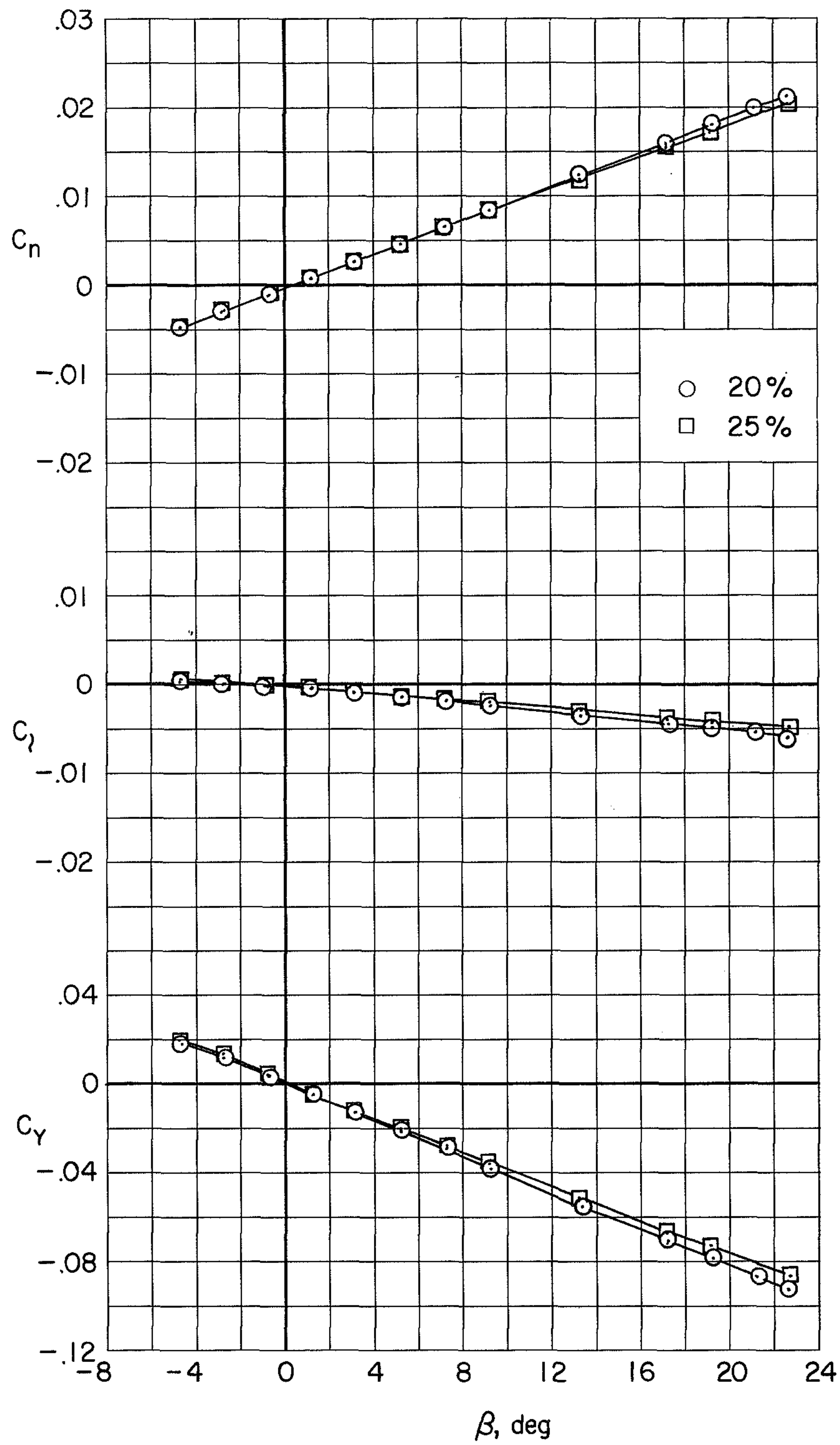

(b) Static lateral-directional characteristics, α = 0.

Figure 6.- Concluded.

[redacted]

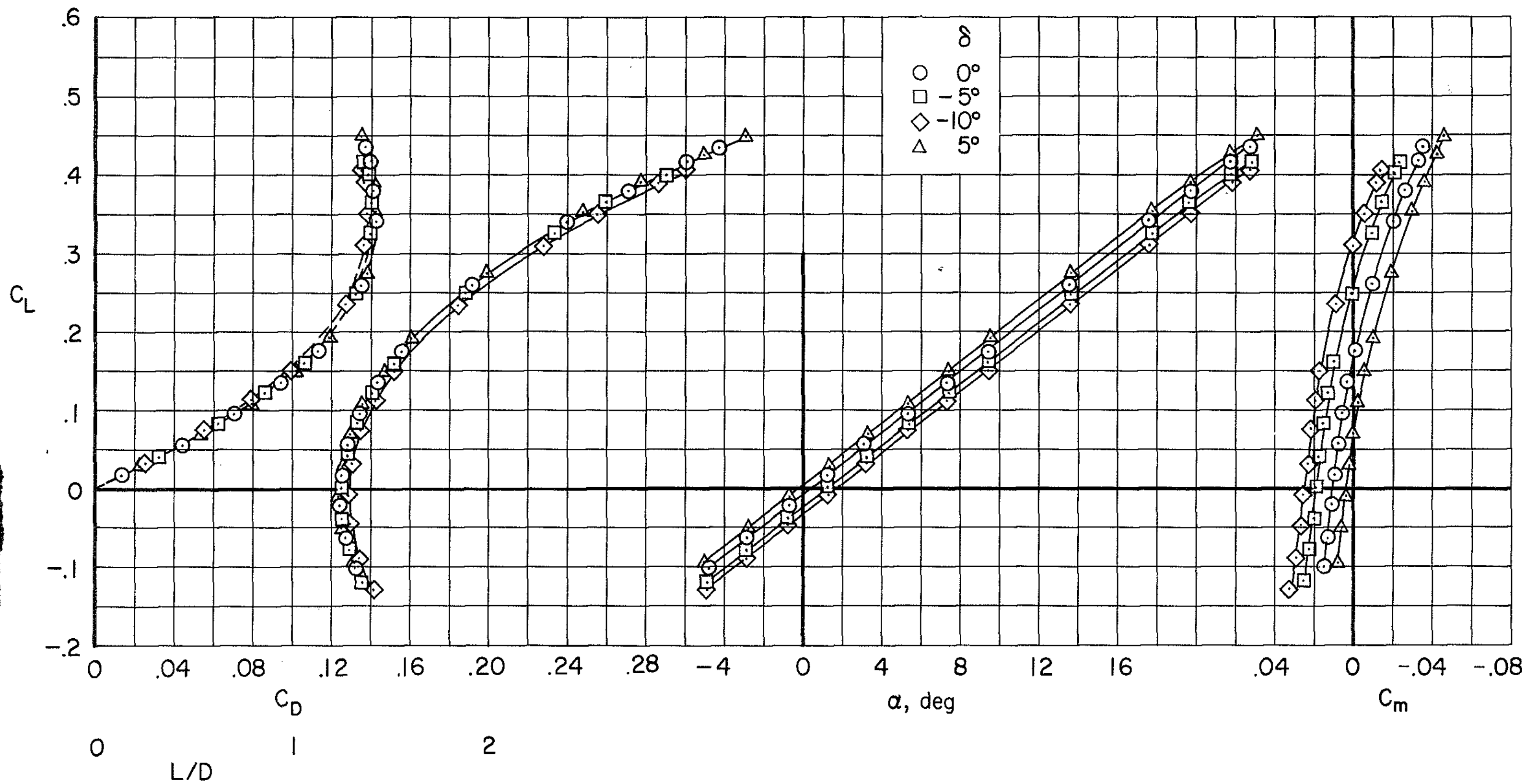

(a) Static longitudinal characteristics.

Figure 7.- Effect of horizontal-control surface deflection on the aerodynamic characteristics of the model with thickness-diameter ratio of 0.225 (20-percent-area horizontal-control surfaces).

[redacted]

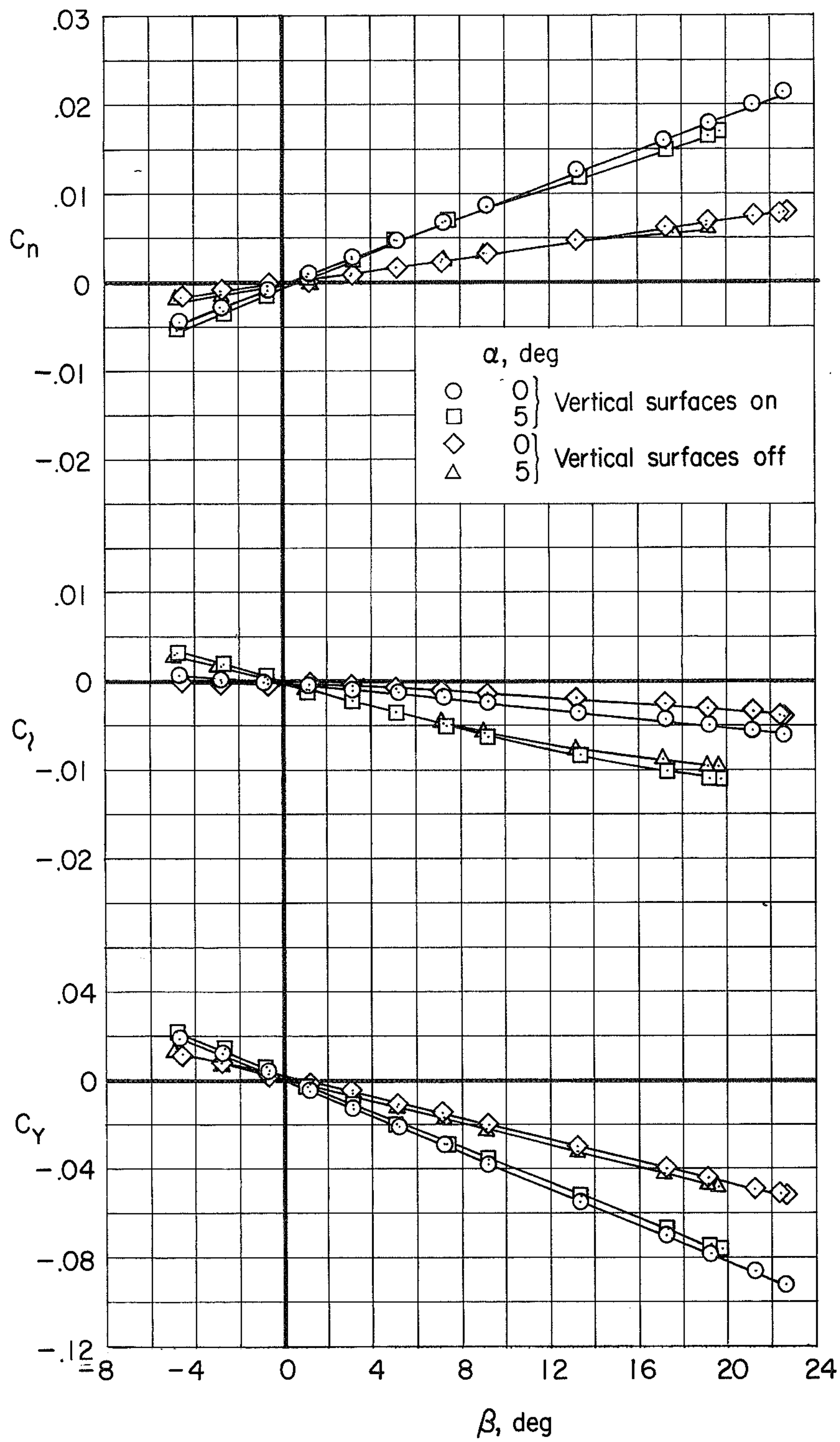

(b) Static lateral-directional characteristics.

Figure 7.- Concluded.

A
4
8
0

[redacted]

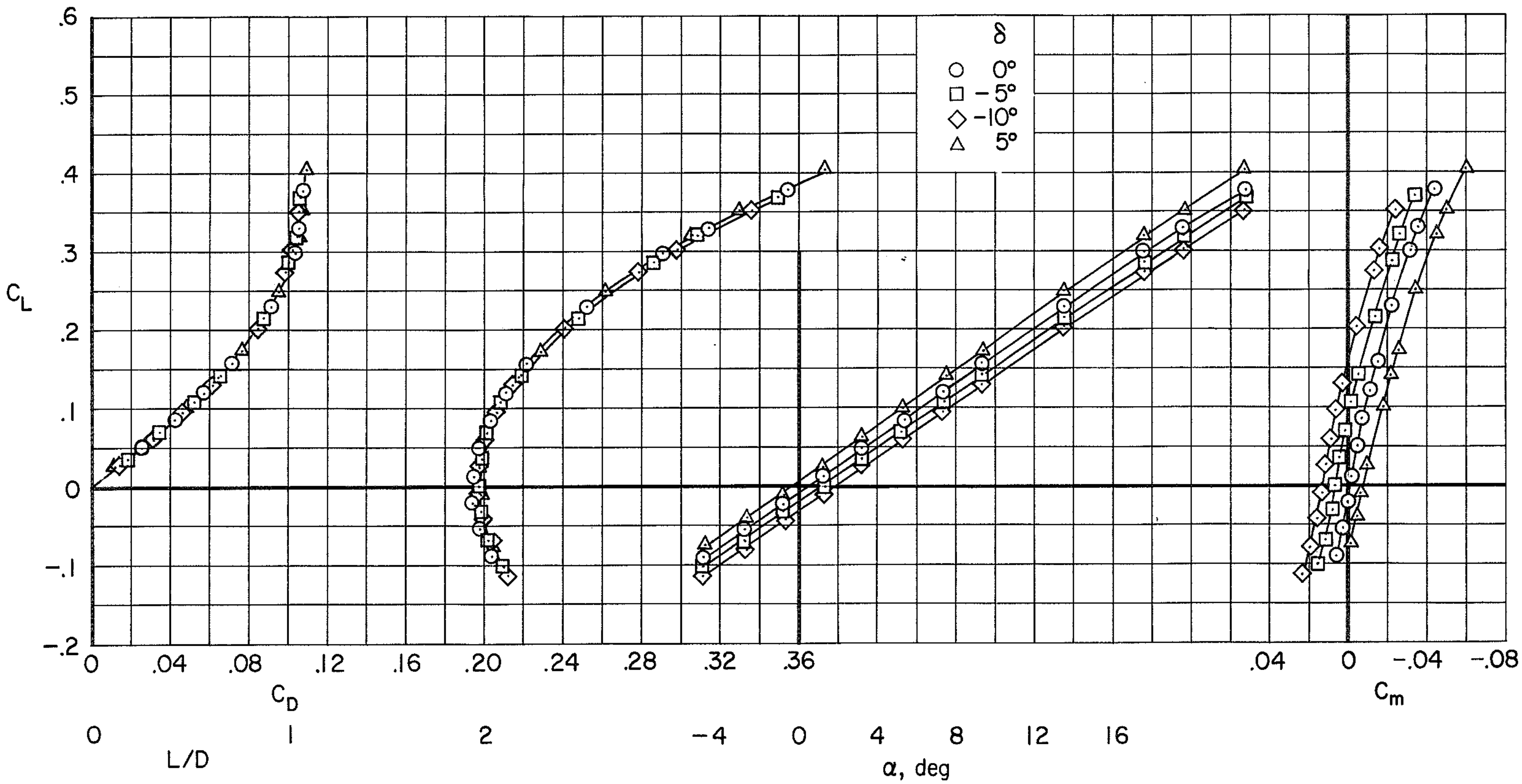

(a) Static longitudinal characteristics.

Figure 8.- Effect of horizontal-control surface deflection on the aerodynamic characteristics of the model with thickness-diameter ratio of 0.325 (25-percent-area horizontal-control surfaces).

[redacted]

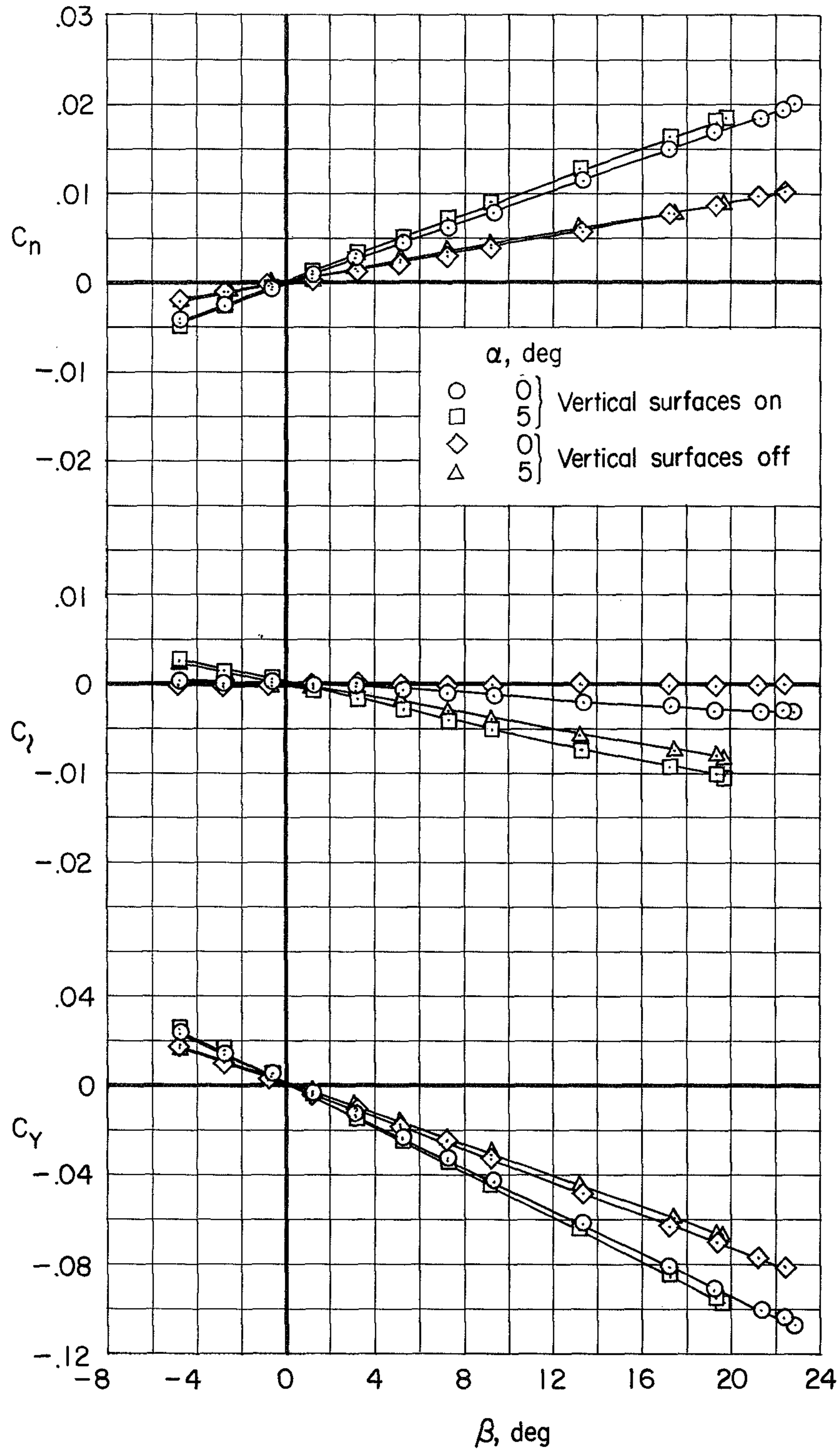

(b) Static lateral-directional characteristics.

Figure 8.- Concluded.

A
4
8
0

[redacted]

DECLASSIFIED

[redacted]

[redacted]

[redacted]

[redacted]